International Journal of Biological Macromolecules 103 (2017) 395–402

Contents lists available at ScienceDirect

International Journal of Biological Macromolecules

journal homepage: www.elsevier.com/locate/ijbiomac

Ultrafast spectroscopy on DNA-cleavage by endonuclease in molecular crowding

Priya Singh [a], Susobhan Choudhury [a], Shreyasi Dutta [a], Aniruddha Adhikari [a], Siddhartha Bhattacharya [b], Debasish Pal [b], Samir Kumar Pal [a,*]

[a] Department of Chemical, Biological & Macromolecular Sciences, S. N. Bose National Centre for Basic Sciences, Block JD, Sector III, SaltLake, Kolkata 700 106, India
[b] Department of Zoology, Uluberia College, University of Calcutta, Uluberia, Howrah 711315, India

ARTICLE INFO

Article history:
Received 23 February 2017
Accepted 14 May 2017
Available online 15 May 2017

Keywords:
Enzymatic activity
DNase I
Molecular crowding
FRET

ABSTRACT

The jam-packed intracellular environments differ the activity of a biological macromolecule from that in laboratory environments (*in vitro*) through a number of mechanisms called molecular crowding related to structure, function and dynamics of the macromolecule. Here, we have explored the structure, function and dynamics of a model enzyme protein DNase I in molecular crowing of polyethylene glycol (PEG; MW 3350). We have used steady state and picosecond resolved dynamics of a well-known intercalator ethidium bromide (EB) in a 20-mer double-stranded DNA (dsDNA) to monitor the DNA-cleavage by the enzyme in absence and presence PEG. We have also labelled the enzyme by a well-known fluorescent probe 8-anilino-1-naphthalenesulfonic acid ammonium salt (ANS) to study the molecular mechanism of the protein-DNA association through exited state relaxation of the probe in absence (dictated by polarity) and presence of EB in the DNA (dictated by Förster resonance energy transfer (FRET)). The overall and local structures of the protein in presence of PEG have been followed by circular dichroism and time resolved polarization gated spectroscopy respectively. The enhanced dynamical flexibility of protein in presence of PEG as revealed from excited state lifetime and polarization gated anisotropy of ANS has been correlated with the stronger DNA-binding for the higher nuclease activity. We have also used conventional experimental strategy of agarose gel electrophoresis to monitor DNA-cleavage and found consistent results of enhanced nuclease activities both on synthetic 20-mer oligonucleotide and long genomic DNA from calf thymus.

1. Introduction

Many *in vivo* enzymatic processes including repression or activation of transcription in gene regulatory network are triggered by binding of proteins to their respective target sites on DNA. However the study of enzyme-DNA interactions have been usually designed as dilute solution experiments, which differ substantially from *in vivo* conditions as 40% volume of cytosol is occupied by a wide variety of macromolecules and solutes [1–3]. Due to this reason, the diffusion of any solutes in intracellular environment is get affected either being reduced or presenting anomalous diffusion at short times [4–8]. Contemporary studies have revealed that macromolecular crowding inside the cell does not only affect diffusion processes but also biochemical reaction processes by inducing the enzyme to undergo protein folding, self-association, or protein-binding processes, which in turn may alter the activity of the enzyme [9–12]. Thus, in order to obtain more accurate rates for enzymatic reactions, it is important to perform the studies of biochemical processes in nature-like microenvironments that try to mimic the effect of macromolecular crowding.

As the quantitative studies of enzyme-DNA interactions within a living cell are challenging, subsequently to mimic the intracellular like environment the high concentration of crowding agents are often used in the *in vitro* studies. For this purpose polyethylene glycol and polysaccharides are often considered as a convenient macromolecular crowder as it is highly soluble in water, it does not precipitate the biological macromolecules used for the study and also it does not bind with the biological macromolecules before and after the reaction [13]. Polymer cosolutes (PEG) usually generate an area inaccessible to other biological macromolecules known as excluded volume and these excluded volume per cosolutes increases as size of cosolutes increases. Apart from this, inclusion of cosolutes causes the decrease of water activity of solution and hence generates an osmotic pressure [14,15]. The dependence of

* Corresponding author.
E-mail address: skpal@bose.res.in (S.K. Pal).

http://dx.doi.org/10.1016/j.ijbiomac.2017.05.058
0141-8130/

the equilibrium binding constant, (K), of the biomolecular reaction on the water activity (a_w) is related to the number of water molecules released (Δn_w) during the reaction represented by the equation, $-\Delta n_w = \frac{\partial \log K}{\partial \log a_w}$. Based on this thermodynamic model, the equilibrium constant of a reaction accompanied by the released of water molecules is found to be 10–100 times higher in solution with water activity less than one [13,16]. The excluded volume of protein in macromolecular crowding can be minimized either by changes in the hydrodynamic volume or *via* changes in its association state [17,18], which are promoted by modulation of the biological equilibria of protein that would affect protein folding, conformational stability, protein-protein interactions and protein nucleic acid interactions [18–20].

Zimmerman and Minton have shown in number of experimental systems which support that crowding promotes molecular association and hence the enzymatic activity [21,22]. In one of the contemporary literature they have shown that in presence of several macromolecules the enzymatic activity of DNA ligases from both rat liver and *Escherichia coli* increases by several orders [23]. Naoki Sugimoto and co-workers have shown that molecular crowding increases the activity of endonucleases but not affect exonucleases [24]. All these studies furnish amendment of catalytic activity of the enzyme as a consequence of molecular crowding. However, the exact role of structure, function and dynamics of enzyme triggering in alteration of enzymatic activity in molecular crowding condition are still poorly understood and a detailed understanding in this field is highly demanding due to the highly compact packing *in vivo* condition.

Here we systemically study the role of molecular crowding such as polyethylene glycol (PEG) on the structure, functionality, substrate binding and dynamic of endonuclease glycoprotein known as bovine pancreatic deoxyribonuclease I (DNase I). DNase I is a secretory glycoprotein that hydrolysed the P-O3′-bond of double-stranded DNA predominantly by single-stranded nicking mechanism under physiological condition in presence of Mg^{2+} and Ca^{2+} [25]. Like many of the non-specific protein-DNA interaction, crystal structure showed that the unspecific DNase I bind tightly in the minor groove and to the sugar-phosphate backbone of both strands of the DNA [25]. In the present study the enzymatic activity of DNase I on the hydrolysis of 20-mer double stranded DNA is found to increase with increasing PEG concentrations through intact structural integrity as revealed from CD in the solution. To corroborate the change in activity and binding of DNase I towards DNA as a function of the concentration of PEG, time resolved fluorescence spectroscopy study was followed. While picosecond resolved transients of EB intercalated to DNA upon interaction with DNase I revealed the extent of DNA cleavage by enzyme in presence and absence of PEG, Förster resonance energy transfer (FRET) studies from 8-anilino-1-naphthalenesulfonic acid ammonium salt (ANS) attached with DNase I to EB intercalated to DNA confirm more efficient binding between DNase I and DNA in presence of PEG. Further, the change in protein dynamics, responsible for the association of DNase I and DNA has been monitored by rotational dynamics as well as picosecond resolved transients of ANS attached to DNase I. We have also confirmed the enhanced activity of DNase I in presence of molecular crowding through conventional way of agarose gel electrophoresis in order to evaluate the hydrolysis of both large (calf thymus) DNA as well as for 20-mer dsDNA.

2. Experimental section

2.1. Chemicals

Bovine pancreatic deoxyribonuclease I (DNase I), 8-anilino-1-naphthalenesulfonic acid ammonium salt (ANS), polyethylene glycol 3350 (PEG), calf thymus DNA and ethidium bromide (EB) were from Sigma-Aldrich (Saint Louis, USA). Tris–HCl, magnesium chloride, agarose, boric acid and EDTA were from SRL (Mumbai, INDIA). Glycerol and calcium chloride were from Merck (Mumbai, INDIA). The chemicals and the proteins are of the highest commercially available purity and were used as received. HPLC-grade oligonucleotide substrates of 20-mer sequences, 5′-GCGTGTAAACGATTCCACGC-3′ and its complement were purchased from Trilink Technologies (San Diego, CA). A 20-mer double-stranded DNA (dsDNA) was prepared by annealing (incubation at 90 °C for 5 min, followed by cooling at 1 °C/min to the reaction temperature) of 5′-GCGTGTAAACGATTCCACGC-3′ and its complement.

2.2. Assay of DNA hydrolysis by nucleases

DNase I was assayed in a buffer of 2.5 mM $MgCl_2$, 0.5 mM $CaCl_2$ and 10 mM Tris–HCl (pH 7.5) at 25 °C. The reactions were performed with 0.5 μM of DNase I and 10 μM dsDNA (20-mer) as a substrate. For quantitative analysis of the hydrolysis reaction of DNase I, the dsDNA was staining with ethidium bromide (EB/DNA = 1:1). DNA hydrolysis was evaluated according to the amount of residual substrate (%). The amount of the residual substrate was estimated as follows:

$$R(\%) = \frac{S_T X 100}{S_0}$$

where, R is residual substrate, S_T is fluorescence intensity of substrate after time T and S_0 is fluorescence intensity of substrate at zero time [24].

For kinetics studies, the dsDNA concentration was varied from 1 to 10 μM for DNase I. The initial rates (v) were estimated from the data for the first 30% of the reaction, where residual substrate varies linearly with time. The values of 1/v were plotted against respective 1/[DNA] to obtain the kinetic parameters (K_m and V_{max}) from Michaelis–Menten equation, $\frac{1}{v} = \frac{K_m}{V_{max}}\frac{1}{[S]} + \frac{1}{V_{max}}$, where [S] indicates substrate concentration. The equations were fitted using Origin 8.5 software [26].

2.3. Experimental details

The steady state absorption and emission spectra were measured with Shimadzu UV-2600 spectrophotometer and Jobin Yvon Fluoromax-3 fluorimeter, respectively. Kinetic measurements were done by time based scan in a Jobin Yvon Fluoromax-3 fluorimeter with a Peltier thermostat maintained at 25 °C, where excitation and emission monochromator were set at 512 nm and 595 nm, respectively. CD spectra of native DNase I and DNase I-DNA complexes in presence and absence of PEG were recorded at pH 7.5 using a JASCO-810 spectrometer. The spectra were collected in the far- UV region (200–350 nm) by a quartz cell with a path length of 1 mm. The sample temperature was maintained at 25 °C using a Peltier thermostat. The electrophoretic mobility of calf thymus DNA and 20-mer dsDNA complexes upon hydrolysis by DNase I in 2.5 mM $MgCl_2$, 0.5 mM $CaCl_2$ and 10 mM Tris–HCl buffer solution (pH 7.5) was determined by gel electrophoresis using 1.5% agarose gels. Experiments were run at 100 V for 15 min in case of calf thymus DNA and 5 min for 20-mer DNA. Since the calf thymus DNA and 20-mer dsDNA were labelled with ethidium bromide, a photograph of the gel was taken under ultraviolet illumination of gel documentation and image analysis system Syngene, UK Model:INGENIUS 3 without staining the gel with ethidium bromide.

All the picosecond resolved fluorescence transients were measured by using commercially available time-correlated single-photon counting (TCSPC) setup with MCP-PMT from Edinburgh instrument, U.K. (instrument response function (IRF) of ~75 ps) using a 375 nm and 409 nm excitation laser source while the flu-

orescence transients of EB and ANS in different systems were measured in 50 ns and 20 ns time window respectively. Further in order to maintain equilibrium during the life time measurement, all the time resolved fluorescence transient of EB-DNA in absence and presence of PEG were taken just after 10 min from the time when it was mixed with DNase I so that the rate of enzymatic reaction could reach toward the saturation. The sample temperature was maintained by a controller from Julabo (Modal 532). Details of the time resolved fluorescence setup have been depicted in our previous reports [27–29]. To estimate the FRET efficiency of energy donor (D) to the different acceptors (A) and hence to determine the distance of the FRET pair (D-A), we have followed the methodology described elsewhere [30–32]. In brief, D-A distance, r, can be calculated from the equation, $r^6 = \frac{R_0^6(1-E)}{E}$, where E is the energy transfer efficiency between donor and acceptor, and R_0 is Förster distance. E was calculated using the equation, $E = 1 - \frac{\tau_{DA}}{\tau_D}$, Where τ_{DA} and τ_D are fluorescence lifetimes of the donor in presence and absence of acceptor. For the fluorescence anisotropy measurements, the emission polarizer was adjusted to be parallel and perpendicular to that of the excitation and collected the fluorescence transients I_{para} and I_{per}, respectively. The anisotropy is defined as, $r(t) = \frac{I_{para} - G*I_{per}}{I_{para} + 2*G*I_{per}}$. The magnitude of G, the grating factor of emission monochromator of the TCSPC system, could be found using a long tail matching technique [28,33].

3. Results and discussion

The kinetics of hydrolysis of the substrate dsDNA-EB by DNase I has been measured by steady state fluorescence technique and is found that the rate of exclusion of the EB from DNA upon hydrolysis by DNase I increases gradually as the concentration of PEG increases in the solution. Fig. 1(a) shows that in absence of PEG the amount of residual dsDNA after 300 s is estimated to be 67%; however it reduced to 57%, 49% and 48% in presence of 5, 10 and 15 wt% PEG [34–36]. To calculate the rate constant and the maximum velocity, we have measured the kinetics at different substrate concentrations. Fig. 1(b) depicts the corresponding Lineweavere-Burk plot for different PEG concentration, where the reciprocal of the reaction velocity (v) is plotted as a function of the reciprocal of the concentration of DNA [29]. The curves produce good linear fits for all the systems and from the slope and intercept of the curves, we have calculated the Michaelise-Menten constant (K_m) and the maximum velocity (V_{max}) for all the systems. The calculated K_m and V_{max} values for the three different PEG concentrations are presented in Fig. 1(c) which clearly indicates that with the increase in PEG concentration, V_{max} increases however, K_m for the enzymatic activities of DNase I for substrate DNA decreases. These kinetic parameters reveal that molecular crowding influences the hydrolytic activity of the DNase I by affecting catalytic activity as well as its binding affinity toward the substrate DNA, indicated by both increase of V_{max} and decrease of K_m [34,37].

In order to reveal whether the changes in catalytic activity induced by PEG are accompanied by alterations in the secondary structures of DNase I, CD spectroscopy were performed. As observed from Fig. 2(a) the aqueous DNase I solution displays CD features with minimum value at 208 and 215 nm (far UV-CD), corroborating the native secondary structures of the enzyme [38] which is observed to be insignificantly perturbed in presence of PEG, indicating that the secondary structure of the enzyme is preserved up to 15 wt% PEG concentration. Inset of Fig. 2(a) symbolize the percentage of α strand and β sheet in free DNase I in absence and presence of 15 wt% PEG which remain almost same in both the cases. To gain insight about the DNA structure perturbation by DNase I, we have next focused on conformational changes of 20-mer DNA, which exhibits two characteristics peaks

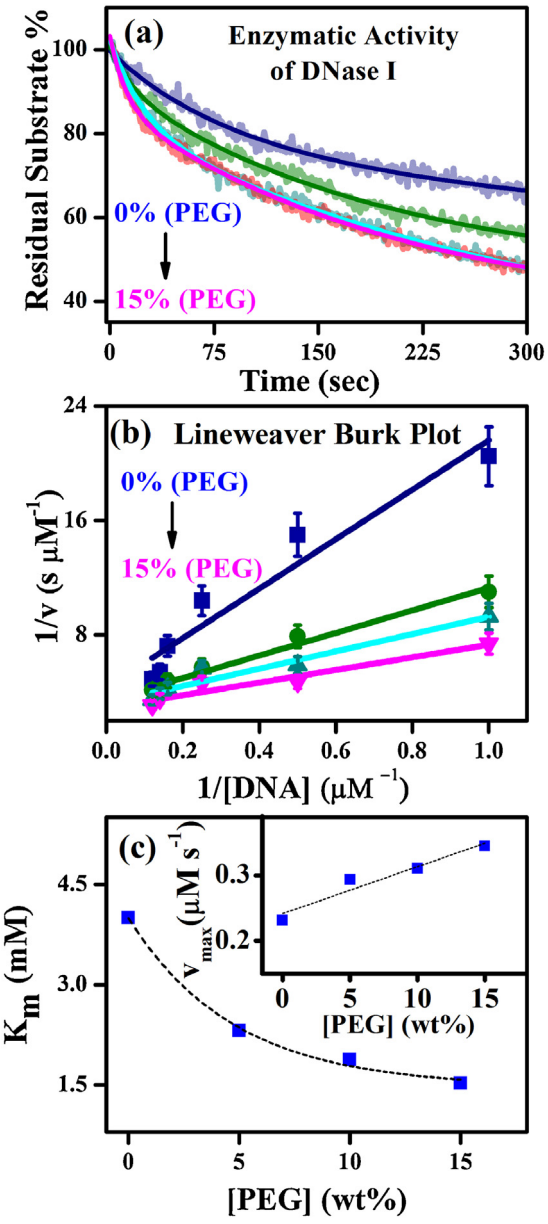

Fig. 1. a) Amount of residual DNA upon hydrolysis by DNase I in the presence of 0, 5, 10 and 15 wt% of PEG. b) A representative Lineweavere-Burk plot for the catalytic activity of DNase I on the substrate DNA in presence of 0, 5, 10 and 15 wt% PEG. c) K_m for the catalytic activity of DNase I on the substrate DNA as a function of PEG concentrations. The plot of V_{max} against PEG concentration is shown in the inset.

(inset of Fig. 2(b)); one positive band around 280 nm complemented to π-π base stacking, and one negative band around 245 nm for hellicity [39]. Upon addition of DNase I the band at 280 nm was insignificantly perturbed however, the band at 245 nm became less negative, this in turn attributed to partial B-to-A DNA transition upon protein interaction [40]. In order to explore the cleavage of DNA in presence and absence of PEG, DNA was intercalated with EB which generated induced CD signal near 303 nm along with and increasing helicity peak of DNA [41] as shown in Fig. 2(b). In presence of PEG, an insignificant decrease in the induced CD spectra at 303 nm was observed may be due to osmotic stress of PEG, while the nature of the spectra remained nearly unchanged, demonstrating that DNA remained in B conformation upon addition of PEG. When DNase I is added to the DNA-EB system, decrease in 303 nm spectra is observed however, a commendable variation has been observed when DNase I is added to DNA-EB system containing 15 wt% of

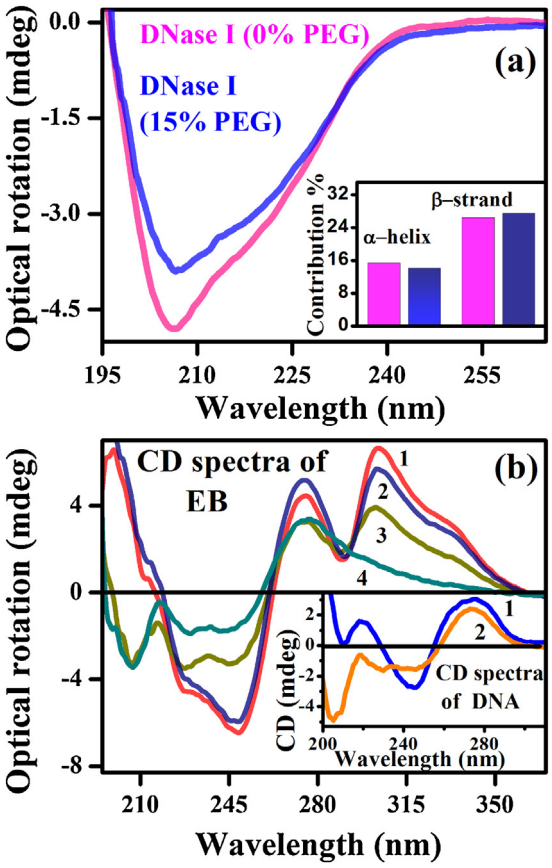

Fig. 2. a) The far UV-CD (circular dichroism) spectra of DNase I at 0 and 15 wt% PEG. Contribution of alpha strand and beta sheet at various wt% PEG is shown in inset. b) Induced CD (circular dichroism) spectra of EB intercalated to DNA in 1) buffer, 2) 15 wt% PEG, 3) complexed with DNase I in buffer and 4) complexed with DNase I in 15 wt% PEG. CD spectra of 1) DNA and 2) DNA-DNase I complex are shown in inset.

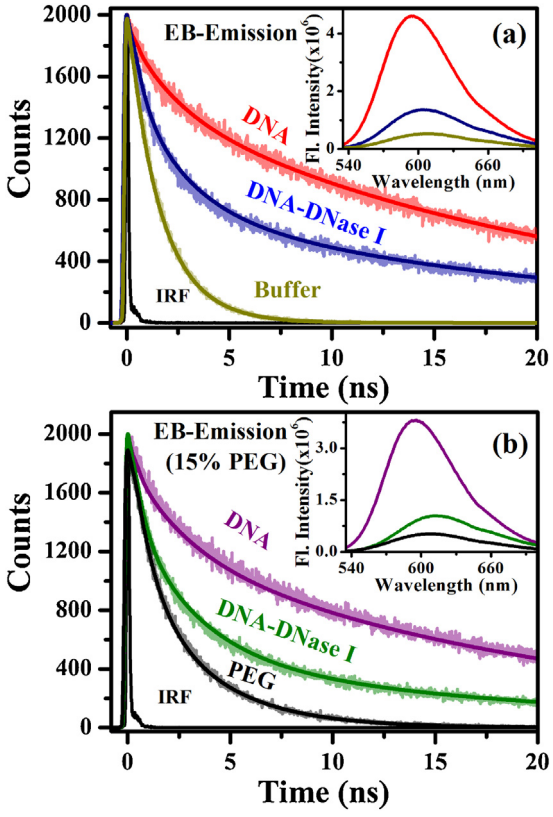

Fig. 3. Picosecond-resolved transient of free EB, EB in DNA and in DNA-DNase I complex in presence of a) 0 wt% PEG and b) 15 wt% PEG. Insets depict the corresponding steady state emission of free EB, EB in DNA and in DNA-DNase I complex.

Table 1
Fluorescence lifetimes of EB in different systems.

system	τ_1 ns [%]	τ_2 ns [%]	τ_3 ns [%]	τ_{avg} ns
DNA	0.21 (27)	2.21 (19)	21.0 (54)	11.9
DNA-DNase I	0.50 (36)	2.57 (35)	21.0 (29)	7.2
DNA-PEG	0.26 (30)	2.70 (23)	20.40 (47)	10.4
DNA-DNase I-PEG	0.51 (42)	3.24 (40)	20.30 (18)	5.2
Buffer	0.47 (20)	1.68 (80)	–	1.4
PEG	0.93 (51)	3.46 (49)	–	2.1

PEG, infers that cleavage has enhanced in presence of PEG. In this light of understanding, altered enzymatic activity offers a unique opportunity for correlating the function with the dynamics. For this reason fluorescence spectroscopic techniques can prove useful to understand bio-macromolecular dynamics over a broad time scale.

The enhanced hydrolysis (V_{max}) of DNA by DNase I in presence of PEG is established by monitoring the picosecond resolved transients of EB intercalated to DNA. The significant decrease in emission intensity and red shift of EB emission maxima in the DNA-DNase I complex compared to EB-DNA in buffer indicates the lowering of the contribution of EB binding to the DNA upon cleavage with DNase I (inset of Fig. 3(a)). Fig. 3(a) shows picosecond resolved transients of EB in buffer and in EB-DNA complexes in absence and presence of DNase I. The tri-exponential fitting of the fluorescence decay of EB in DNA revealing ~21 ns as major component (54%) indicates that most of the EB is intercalated to the DNA [42]. However, upon hydrolysis of EB-DNA complexes by DNase I the contribution of longer decay component ~21 ns (29%) decreases considerably, reflecting significant cleavage of DNA by DNase I in buffer solution as shown in Table 1. In order to investigate the effect of PEG in hydrolysis of DNA, picosecond resolved transients of all the system are studied in presence of 15 wt% PEG, shown in Fig. 3(b). It is observed that the maximum population of the dye intercalated to the DNA in presence of PEG is slightly decreased (~21 ns (47%)) in contrast to that in DNA in buffer solution (~21 ns (54%)) which occurred may be due to osmotic stress created by PEG. The transient of EB in DNA upon hydrolysis by DNase I in presence of PEG shows that the contribution of a longer time component ~21 ns (18%) is extensively get lower than that of DNA in buffer solution (21 ns (29%)), corroborates the higher cleavage in presence of PEG. Inset of Fig. 3(b) shows the corresponding steady state emission of EB in DNA and DNA-DNase I complex in presence of PEG. It should be noted that decrease in emission intensity and more red shift of EB emission maxima in the DNA-DNase I complex in presence of PEG compared to EB in DNA-DNase I complex in buffer revealing the further reduction of the contribution of EB binding to the DNA upon hydrolysis in presence of PEG.

The binding affinity and dynamics of DNase I with DNA are monitored by using a biologically relevant probe 8-anilino-1-naphthalenesulfonic acid ammonium salt (ANS) which binds selectively to the enzymes in their hydrophobic sites [43]. The excitation spectrum of ANS in buffer shows a peak at 356 nm, which remains same when formed complexed with DNase I, however, the emission spectrum of the ANS-DNase I complex shows a blue shift (60 nm) compared to that in buffer as shown in Fig. 4(a), indicate interaction of ANS to the hydrophobic sites of protein. Picosecond-resolved transients of ANS in buffer, DNase I-bound ANS and its complex with DNA are shown in Fig. 4(b). ANS in complexed with DNase I show essentially fluorescence decays of average time constants 8.12 ns which is much slower than ANS in

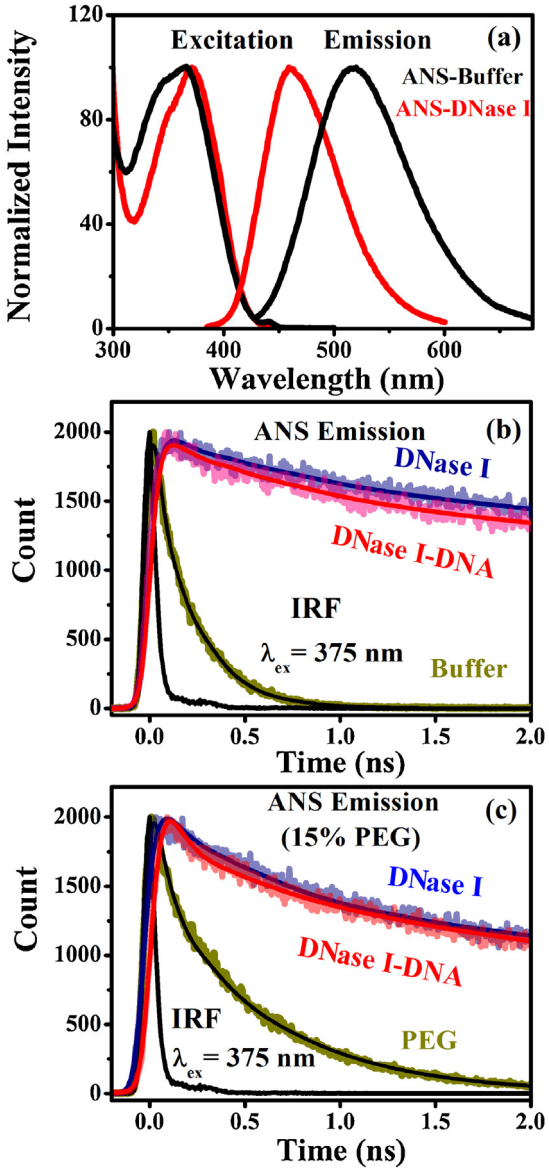

Fig. 4. a) Steady state excitation and emission spectra of ANS in buffer and in complex with DNase I. Time-resolved transients of free ANS, ANS bound to DNase I in the presence and absence of DNA are shown in presence of b) 0 wt% PEG and c) 15 wt% PEG.

Table 2
Fluorescence lifetimes of ANS in different systems.

system	τ_1 ns [%]	τ_2 ns [%]	τ_3 ns [%]	τ_{avg} ns
DNase I	0.15 (32)	1.52 (13.4)	14.42 (54.6)	8.12
DNaseI-DNA	0.14 (33.8)	1.32 (16.1)	13.90 (50.1)	7.22
DNase I-DNA-EB	0.11 (39.3)	1.15 (27.3)	11.74 (33.4)	4.28
DNase I-PEG	0.14 (32.6)	1.07 (27.2)	13.22 (40.2)	5.66
DNase I-PEG-DNA	0.14 (35.4)	1.16 (24.4)	12.59 (40.2)	5.39
DNase I-PEG-DNA-EB	0.13 (34.7)	0.83 (46.9)	10.85 (18.4)	2.43
Buffer	0.23 (100)	–	–	0.23
PEG	0.37 (48)	0.86 (52)	–	0.63

buffer (0.23 ns). The longer life time of ANS-DNase I is observed to be similar to that of the ANS-DNase I-DNA complex, revealing the fact that ANS molecules are not detached from DNase I upon complexation (Table 2). Further, in order to understand the effect of confinement on the fate of ANS bound DNase I, similarly the picosecond transients of ANS in all the systems were performed in presence of PEG. The average fluorescence decays time constants

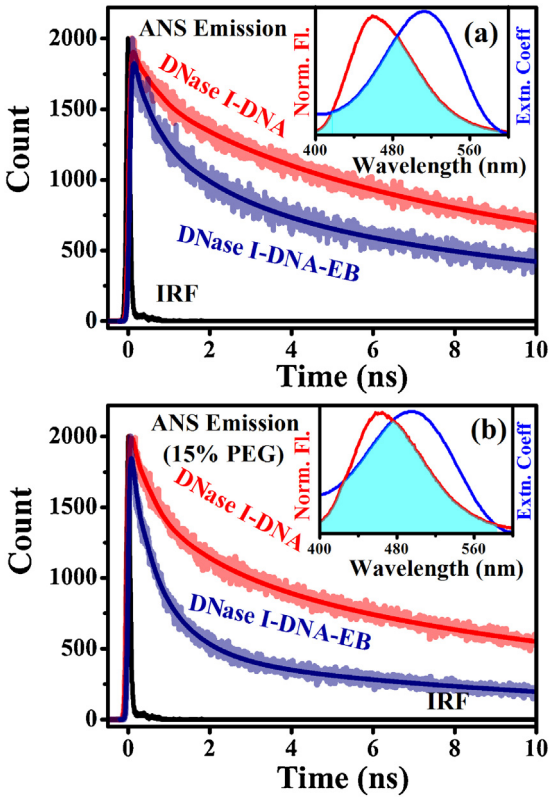

Fig. 5. Picosecond-resolved transients of the donor (ANS-DNase I-DNA complex) in the absence and presence of the acceptor (EB) in DNA in a) 0 wt% PEG and b) 15 wt% PEG. Insets depict the corresponding spectral overlap between donor (ANS-DNase I-DNA complex) emission and acceptor (ANS-DNase I with EB-bound DNA) absorbance.

of ANS in complexed with DNase I was found to be 5.66 ns, whereas an insignificant change in life time of ANS-DNase I-DNA in presence of PEG was observed shown in Fig. 4(c).

The intactness of ANS in DNase I upon complex with DNA has enabled us to carry out Förster resonance energy transfer (FRET) studies from the donor, ANS in DNase I, to another dye (acceptor), ethidium bromide (EB), intercalated in the DNA, which also corroborates the binding between enzyme and DNA. The significantly large spectral overlap ($2.58 \times 10^{14}\ M^{-1}\ cm^{-1}\ nm^4$) of the donor (ANS) emission and acceptor (EB) absorption spectra favours energy transfer from the donor to the acceptor as shown in inset of Fig. 5(a). The picosecond resolved transient (Fig. 5(a)) of the ANS in DNase I-DNA complex reveals an average decay time constant of 7.22 ns and 4.28 ns in the absence and presence of the acceptor (EB), respectively. The efficiency of energy transfer and donor–acceptor distance was calculated to be 40% and 28.7 Å, respectively. To gain insight into the effect of PEG in the binding between DNase I and DNA, we have executed the similar FRET study in presence of PEG. The absorption spectrum of EB bound to DNA has almost same spectral overlap with the emission spectrum of ANS in DNase I in presence of PEG (inset of Fig. 5(b)). The fluorescence transient of ANS in DNase I in 15%wt PEG is quenched in presence of EB interacted to DNA as shown in Fig. 5(b) and Table 2 and the efficiency of energy transfer and ANS- EB distances in presence of PEG is found to be 54%, and 22.9 Å, respectively. The higher efficiency of energy transfer leading to shorter FRET distance in presence of PEG corroborates higher binding between DNase I and DNA compared to that in absence of PEG, which is also consistent with our kinetics studies.

In order to gain insight in the basis for higher binding between DNase I-DNA in presence of PEG, we compare the average life-

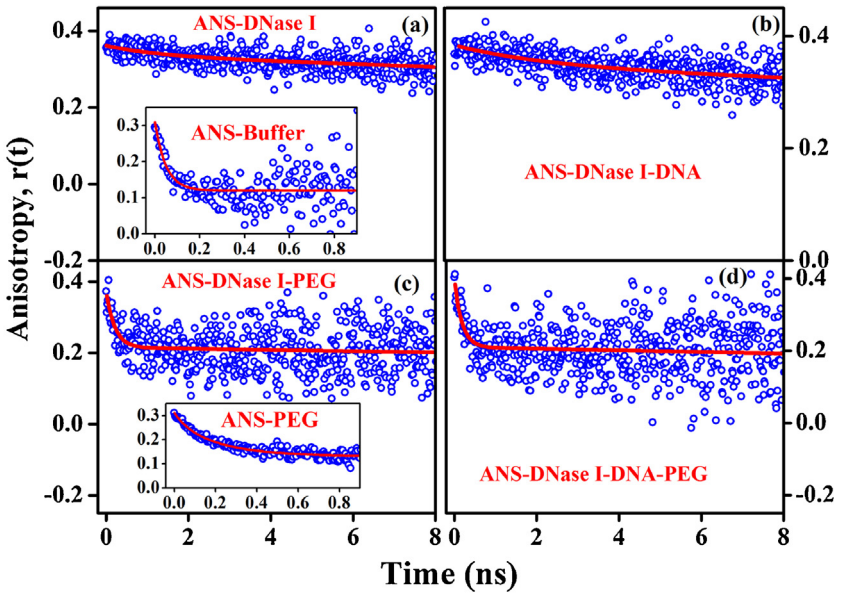

Fig. 6. Time-resolved fluorescence anisotropy of ANS bound to DNase I in presence of a). 0 wt% PEG and c) 15 wt% PEG. Inset shows the corresponding time-resolved anisotropy of free ANS. Time-resolved anisotropy of ANS bound to DNase I in the presence of DNA in b) 0 wt% PEG and d) 15 wt% PEG.

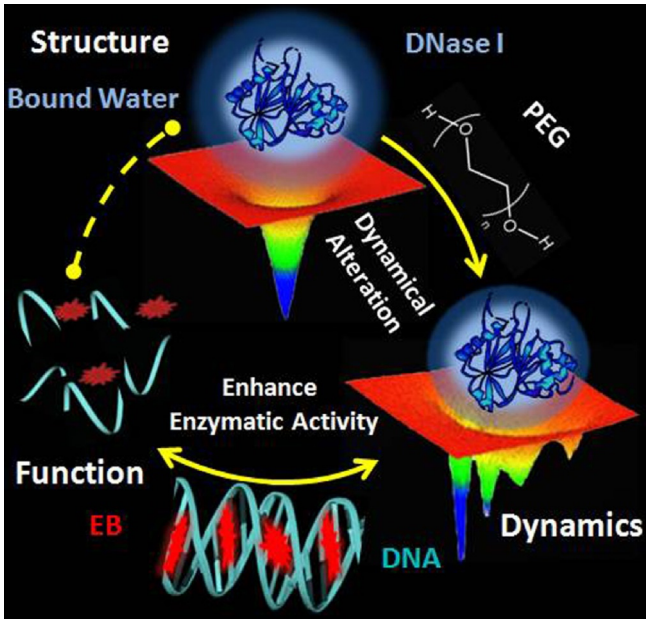

Scheme 1. Schematic representation of the correlation between dynamics and function of DNase I in presence of PEG as molecular crowding.

time of ANS bound to DNase I in presence and absence of PEG and found that the contribution of average time constant characteristic of ANS-DNase I adduct, decreases from 8.12 ns in the buffer to 5.66 ns in presence of 15 wt% PEG (as shown in Fig. 4(a) and (b)). The observation is consistent with the fact that faster dynamics at the higher concentration of PEG suggests thinning of the hydration water shell around the enzyme due to decreased water activity and hence leads to higher binding between DNase I-DNA, which accelerates the hydrolysis of DNA (Scheme 1) [15]. Bagchi et al. earlier proposed the presence of at least two types of water molecules at the protein surface and these water molecules remain in a dynamic equilibrium with the bulk or free type water molecules ($Water_{surfacebound} \leftrightarrow Water_{bulk}$) [44–46]. This equilibrium between the bound and bulk water is sensitive to the change in the microenvironment of the protein, *e.g.* temperature, pressure, additives *etc.* Hence, addition of PEG produces an osmotic stress in the hydration layer, which in turn shifts the equilibrium towards a less hydrated conformation and also increases the contribution of faster moving bulk water molecules around the enzyme's surface. This explains the observed decrease in the average time constant of ANS bound to DNase I with increased in PEG concentration.

The hydration shell formed by water molecules in the close vicinity of a protein molecule is crucial for protein structure and folding and defines the substrate binding, and molecular recognition [47]. Changes in the protein hydration are known to be related to changes in protein catalytic activity and also have a profound effect on protein conformational stability and dynamics [47–51]. As in our studies the changes in catalytic activity induced by PEG are not accompanied by change in conformation hence, in order to confirm the modification of the enzyme's dynamics with the addition of PEG, we measured the temporal anisotropy decay, r(t), of the probe ANS bound to DNase I in buffer and in presence of 15 wt% PEG concentrations. ANS in buffer exhibits a fast single exponential rotational decay [52] (inset of Fig. 6(a)), on the other hand the rotational relaxation of ANS bound to DNase I and upon complexation with DNA has been found to be bi-exponential with comparable time constant, attributing that dynamics of DNase 1 was insignificantly perturbed when it form complex with DNA (Fig. 6(a) and (b)). Further, with the addition of PEG to ANS-DNase I complex, the components of local and global tumbling motion of probe get faster indicating a greater contribution from the bulk type of water molecules in the proximity of the probe. However, ANS is still bound to the enzyme is evident from the presence of a slow component which was not found in 15 wt% PEG solution without the enzyme as shown in inset of Fig. 6(c) and Table 3. Similarly when ANS-DNase I formed complex with DNA in presence of PEG the rotational relaxation time constant of ANS was found to be insignificantly perturb in comparison to the rotational relaxation time constant of probe in ANS-DNase I complex (Fig. 6(d)). This observation clearly indicates that, flexibility of ANS attached to hydrophobic core of DNase I is much higher in presence of PEG compared to in absence of PEG. It is worth mentioning that the result obtain from rotational dynamic of enzymes is also corroborated by time resolved measurement.

Table 3
Rotational time constants of ANS at the enzyme (DNase I) surface at various systems.

system	τ_1 ns [%]	τ_2 ns [%]	τ_{avg} ns
ANS-DNase I	1.32 (11.3)	45 (88.7)	39.6
ANS-DNase I-DNA	0.9 (14.7)	45 (85.3)	38.4
ANS-DNase I-PEG	0.20 (66.4)	40 (33.6)	13.5
ANS-DNase I-DNA-PEG	0.13 (70.8)	40 (29.2)	11.7
Buffer	0.07 (100)	–	0.07
PEG	0.19 (100)	–	0.19

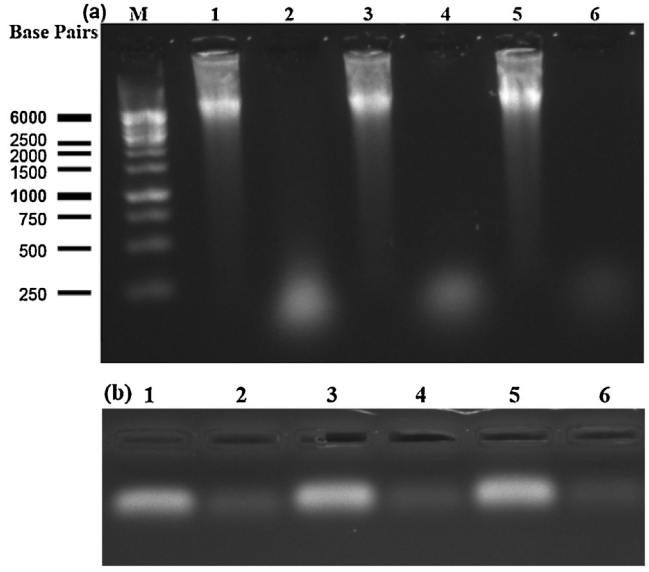

Fig. 7. a) Hydrolysis of calf thymus DNA by DNase I at 25 °C. Lane M shows the DNA size marker. Lanes 1, 3 and 5 show DNA in presence of 0, 5 and 15 wt% PEG. Lanes 2, 4 and 6 shows hydrolysis by DNase I in the presence of 0, 5 and 15 wt% PEG. b) Hydrolysis of a short oligonucleotide DNA (20-mer dsDNA) by DNase I at 25 °C. Lanes 1, 3 and 5 shows DNA in presence of 0, 5 and 15 wt% PEG. Lanes 2, 4 and 6 shows hydrolysis by DNase I in presence of 0, 5 and 15 wt% PEG.

The effect of molecular crowding on the catalytic activity of DNase I was also analysed using agarose gel electrophoresis. Initially we examined the hydrolysis of larger genomic DNA (calf thymus) by DNase I at 25 °C in absence and presence of different PEG concentration. Before hydrolysis by DNase I the migration of substrate DNA in absence and presence of 5 and 15 wt% PEG were found to be same (Fig. 7(a)), validate PEG does not significantly affect the stability of DNA (lane 1, 3 and 5). Migration of bands were found to be faster (lane 2, 4 and 6) upon hydrolysis with DNase I with respect to substrate corroborate the formation of degraded product from the substrate. The diffused band of degraded product in absence of PEG were found to be smeared and of higher intensity, however, the smearing and intensity of bands were found to be decreased as the PEG wt% was increased corroborate the formation of higher degraded product from the substrate in presence of molecular crowding. To evaluate the effect of molecular crowding on hydrolysis of short DNA using agarose gel electrophoresis, 20-mer dsDNA was used as a substrate shown in Fig. 7(b). Like genomic DNA, the migration of 20-mer dsDNA was also found to be same in absence and presence of 5 and 15 wt% PEG (lane 1, 3 and 5). Upon hydrolysis by DNase I the intensity of substrate DNA was decreased as concentration of molecular crowding was increasing (lane 2, 4 and 6). The result shows that dsDNA hydrolysis by DNase I was greatly enhanced by the addition of 5 and 15 wt% PEG. Overall, molecular crowding increases the cleavage yield of DNase I not only for the large DNA (calf thymus) but also for the short (20-mer) DNA oligonucleotide.

4. Conclusions

Our results reveal that the enzymatic activity of DNase I has been increased in presence of a molecular crowding agent, PEG 3350. While, steady state and ultrafast time resolved spectroscopy on a florescence probe EB intercalated to substrate DNA reveal the hydrolysis of the substrate by DNase I, the spectroscopic information including picosecond resolved fluorescence polarization gated studies on the enzyme-bound fluorescence probe ANS shows enhanced surface flexibility of DNase I in the presence of PEG. The reduced water activity at the enzyme surface due to osmotic stress of the molecular crowding agent enhancing the dynamical flexibility of the enzyme is concluded to increase the DNA binding eventually accelerate the hydrolysis reaction of DNase I. In summary the study attempts to unravel the molecular picture of DNA hydrolysis by an endonuclease in presence of an osmotic stress generating molecular crowding agent. A clear correlation of the flexibility of the endonuclease with the rate of DNA hydrolysis within the overall structural integrity of the enzyme has also been established.

Acknowledgements

SC thanks CSIR (India) for the research fellowships. Financial grants (SB/S1/PC-011/2013) from DST (India) and (2013/37P/73/BRNS) from DAE (India) are gratefully acknowledged. Authors also thank DBT (WB)-BOOST scheme for financial grant, 339/WBBDC/1P-2/2013.

References

[1] A.B. Fulton, Cell 30 (1982) 345–347.
[2] R.J. Ellis, Trends Biochem. Sci. 26 (2001) 597–604.
[3] L. Homchaudhuri, N. Sarma, R. Swaminathan, Biopolymers 83 (2006) 477–486.
[4] N. Muramatsu, A.P. Minton, Proc. Natl. Acad. Sci. U. S. A. 85 (1988) 2984–2988.
[5] M. Arrio-Dupont, G. Foucault, M. Vacher, P.F. Devaux, S. Cribier, Biophys. J. 78 (2000) 901–907.
[6] C. Balcells, I. Pastor, E. Vilaseca, S. Madurga, M. Cascante, F. Mas, J. Phys. Chem. B 118 (2014) 4062–4068.
[7] M. Weiss, M. Elsner, F. Kartberg, T. Nilsson, Biophys. J. 87 (2004) 3518–3524.
[8] H.-X. Zhou, G. Rivas, A.P. Minton, Annu. Rev. Biophys. 37 (2008) 375.
[9] N. Kozer, G. Schreiber, J. Mol. Biol. 336 (2004) 763–774.
[10] A.P. Minton, J. Pharm. Sci. 94 (2005) 1668–1675.
[11] H. Dong, S. Qin, H.-X. Zhou, PLoS Comput. Biol. 6 (2010) e1000833.
[12] N. Chebotareva, B. Kurganov, N. Livanova, Biochemistry (Mosc.) 69 (2004) 1239–1251.
[13] S.-i. Nakano, D. Miyoshi, N. Sugimoto, Chem. Rev. 114 (2013) 2733–2758.
[14] V. Parsegian, R. Rand, D. Rau, Proc. Natl. Acad. Sci. U. S. A. 97 (2000) 3987–3992.
[15] M.J. Blandamer, J.B. Engberts, P.T. Gleeson, J.C.R. Reis, Chem. Soc. Rev. 34 (2005) 440–458.
[16] B. Schneider, H.M. Berman, Biophys. J. 69 (1995) 2661.
[17] D. Homouz, M. Perham, A. Samiotakis, M.S. Cheung, P. Wittung-Stafshede, Proc. Natl. Acad. Sci. U. S. A. 105 (2008) 11754–11759.
[18] A.P. Minton, Curr. Opin. Struct. Biol. 10 (2000) 34–39.
[19] D.K. Eggers, J.S. Valentine, Prot. Sci. 10 (2001) 250–261.
[20] E. Bismuto, P.L. Martelli, A. De Maio, D.G. Mita, G. Irace, R. Casadio, Biopolymers 67 (2002) 85–95.
[21] S.B. Zimmerman, Biochim. Biophys. Acta 1216 (1993) 175–185.
[22] S.B. Zimmerman, A.P. Minton, Annu. Rev. Biophys. Biomol. Struct. 22 (1993) 27–65.
[23] S.B. Zimmerman, B.H. Pheiffer, Proc. Natl. Acad. Sci. U. S. A. 80 (1983) 5852–5856.
[24] Y. Sasaki, D. Miyoshi, N. Sugimoto, Nucleic Acids Res. 35 (2007) 4086–4093.
[25] M. Gueroult, D. Picot, J. Abi-Ghanem, B. Hartmann, M. Baaden, PLoS Comput. Biol. 6 (2010) e1001000.
[26] Y. Huang, B. s. Freise, J. Am. Chem. Soc. 115 (1993) 3396.
[27] S. Choudhury, G. Naiya, P. Singh, P. Lemmens, S. Roy, S.K. Pal, ChemBioChem 17 (2016) 605–613.
[28] S.S. Narayanan, S.K. Pal, Langmuir 23 (2007) 6712–6718.
[29] P.K. Verma, S. Rakshit, R.K. Mitra, S.K. Pal, Biochimie 93 (2011) 1424–1433.
[30] J.R. Lakowicz, Principles of Fluorescence Spectroscopy, Springer Science & Business Media, 2013.
[31] S. Choudhury, P.K. Mondal, V. Sharma, S. Mitra, V.G. Sakai, R. Mukhopadhyay, S.K. Pal, J. Phys. Chem. B 119 (2015) 10849–10857.

[32] P. Singh, S. Choudhury, G.K. Chandra, P. Lemmens, S.K. Pal, J. Photochem. Photobiol. B: Biol. 157 (2016) 105–112.
[33] S. Choudhury, S. Batabyal, T. Mondol, D. Sao, P. Lemmens, S.K. Pal, Chem. Asian J. 9 (2014) 1395–1402.
[34] S.B. Zimmerman, B. Harrison, Proc. Natl. Acad. Sci. U. S. A. 84 (1987) 1871–1875.
[35] J.R. Wenner, V.A. Bloomfield, Biophys. J. 77 (1999) 3234–3241.
[36] X. Su, C. Zhang, X. Zhu, S. Fang, R. Weng, X. Xiao, M. Zhao, Anal. Chem. 85 (2013) 9939–9946.
[37] M.T. Morán-Zorzano, A.M. Viale, F.J. Muñoz, N. Alonso-Casajús, G.G. Eydallín, B. Zugasti, E. Baroja-Fernández, J. Pozueta-Romero, FEBS Lett. 581 (2007) 1035–1040.
[38] K. Ajtai, S.Y. Venyaminov, FEBS Lett. 151 (1983) 94–96.
[39] Y.M. Evdokimov, T. Pyatigorskaya, O. Polyvtsev, N. Akimenko, V. Kadykov, D.Y. Tsvankin, Y.M. Varshavsky, Nucleic Acids Res. 3 (1976) 2353–2366.
[40] C. N'Soukpoe-Kossi, S. Diamantoglou, H. Tajmir-Riahi, Biochem. Cell Biol. 86 (2008) 244–250.
[41] D. Dalglkish, A. Peacocke, G. Fey, C. Harvey, Biopolymers 10 (1971) 1853–1863.
[42] R. Sarkar, S.K. Pal, Biopolymers 83 (2006) 675–686.
[43] S. Choudhury, S. Batabyal, P.K. Mondal, P. Singh, P. Lemmens, S.K. Pal, Chem. Eur. J. 21 (2015) 16172–16177.
[44] N. Nandi, B. Bagchi, J. Phys. Chem. B 101 (1997) 10954–10961.
[45] S.K. Pal, J. Peon, B. Bagchi, A.H. Zewail, ACS Publications, 2002.
[46] Y. Qin, L. Wang, D. Zhong, Proc. Natl. Acad. Sci. 113 (2016) 8424–8429.
[47] J. Partridge, P.R. Dennison, B.D. Moore, P.J. Halling, Biochim. Biophys. Acta 1386 (1998) 79–89.
[48] Y. Pocker, Cell. Mol. Life Sci. 57 (2000) 1008–1017.
[49] J. Kornblatt, M. Kornblatt, Int. Rev. Cytol. 215 (2002) 49–73.
[50] L. Yang, J.S. Dordick, S. Garde, Biophys. J. 87 (2004) 812–821.
[51] P.J. Halling, Philos. Trans. R. Soc. Lond. B: Biol. Sci. 359 (2004) 1287–1297.
[52] S.K. Pal, J. Peon, A.H. Zewail, Proc. Natl. Acad. Sci. U. S. A. 99 (2002) 15297–15302.